Impact-Compression-Morphology Relationship in Polyolefin Foams

Bureau, Martin N.; Champagne, Michel F.; Gendron, Richard

Publisher's version / Version de l'éditeur:
https://doi.org/10.1177/0021955X05050218
Journal of Cellular Plastics, 41, 1, pp. 73-85, 2005-01-01

Journal of Cellular Plastics
http://cel.sagepub.com/

Impact-Compression-Morphology Relationship in Polyolefin Foams

Martin N. Bureau, Michel F. Champagne and Richard Gendron

Journal of Cellular Plastics 2005 41: 73
DOI: 10.1177/0021955X05050218

The online version of this article can be found at:
http://cel.sagepub.com/content/41/1/73

Published by:
SAGE
http://www.sagepublications.com

Impact–Compression–Morphology Relationship in Polyolefin Foams*

MARTIN N. BUREAU,† MICHEL F. CHAMPAGNE
AND RICHARD GENDRON
Industrial Materials Institute
National Research Council Canada
75 de Mortagne Blvd., Boucherville
Québec, J4B 6Y4, Canada

ABSTRACT: The relationship between the morphology and the mechanical properties of polyethylene (PE) foams has been studied. Experiments have been made on closed cell low density foams at low testing speed as well as in impact conditions. A careful characterization of the cell size distribution and anisotropy was performed and related to the foams mechanical response. The results indicate that the mechanical response of the foams is anisotropic and can be expressed as a function of the foam morphology, using a unique morphological parameter taking into account the cell size in the appropriate direction and foam density. Previously developed for polystyrene foams, the use of this parameter is thus successfully extended to PE-based foams.

KEY WORDS: foams, polyethylene, mechanical behavior, compression, impact, morphology, predictions.

INTRODUCTION

Foams, as engineering materials, are used in all industrial sectors and represent an extraordinary class of materials, due to their properties extending beyond the limits of all other classes of engineering

*This revised paper was presented in its original form at the *Annual Technical Conference ANTEC 2004*, Chicago IL, May 16–20 2004, and the copyright is held by the Society of Plastics Engineers.
†Author to whom correspondence should be addressed.
E-mail: martin.bureau@cnrc-nrc.gc.ca

0021-955X/05/01 0073–13 $10.00/0 DOI: 10.1177/0021955X05050218

materials. A great challenge in engineering foams is to address specific requirements such as specific weight and cost, while answering functional requirements such as properties. In their textbook [1], Gibson and Ashby have developed an approach to correlate the mechanical performance of foams to their density, based on *Optimization Theory for Materials Selection in Design* [2]. According to the latter, semi-analytical equations of the fundamental mechanical properties of foams such as Young's modulus, E, and the yield strength, σ_y, have been developed. In uniaxial compression, these two properties can be expressed as follows:

$$\frac{E}{E_o} = \phi^2 \rho_r^2 + (1-\phi)\rho_r + \frac{p_i(1-2\nu)}{E_o(1-\rho_r)} \tag{1}$$

$$\frac{\sigma_y}{\sigma_o} = 0.3\rho_r^{1.5} + (1-\phi)\rho_r + \frac{(p_i - p_{\text{at}})}{\sigma_o} \tag{2}$$

where, the subscript 'o' refers to the unfoamed polymer properties, ρ_r is the relative density of the foam, $1-\phi$ is the fraction of solid in the cell faces, p_i and p_{at} are the gas pressure in the foam cells and the atmospheric pressure, and ν is the Poisson's ratio. Since most of the material is concentrated in the cell struts and edges, Equations (1) and (2) can be simplified to their first term provided the Poisson's ratio is close to that of the dense solid ($\nu \approx 0.3$), and the internal cell pressure equals the atmospheric pressure. This explains why foam properties are generally expressed as normalized with respect to their solid counterpart values and plotted against their relative density.

Equations (1) and (2) predict that foams with similar density have the same properties, with no respect to cell size and cell orientation, which obviously does not represent the true foam behavior. A refinement of the description of the mechanical behavior of foams with respect to their characteristics of their morphology, namely their cell size, has been proposed, based on the use of the ratio of density to average cell diameter, ρ/d, instead of simply using the density [3]. The compressive properties and impact properties of commercially available closed-cell PS foams have been expressed as a function of this single microstructural parameter ρ/d, with limited data scatter, according to the following:

$$E = c_1 \cdot (\rho/d)^n \tag{3}$$

$$\sigma_y = c_2 \cdot (\rho/d)^m \tag{4}$$

where n and m are constants equal to 1, and c_1 and c_2 are proportionality constants. Equations (3) and (4) suggest that the mechanical

performance of a foam could be maintained at a lower density by decreasing its average cell size, or inversely that improved mechanical performance should be anticipated with smaller average cell size. Such a result could represent obvious economic advantages and supports to some extent claims related to microcellular foams (MCFs) [4].

While good agreement was observed for PS foams, the proposed methodology to relate mechanical properties and microstructure of foams with a microstructural parameter ρ/d requires validation for other materials, and over a wider range of densities. It is the objective of this work to provide further ground to this approach by applying it to PE foams.

EXPERIMENTAL

Two series of PE foams, kindly provided by Dow Chemical and Sealed Air, were studied. The first series (Dow's Ethafoams) has a nominal density ranging from 28 to 102 kg/m^3, while the other (made specifically for this work by Sealed Air) exhibits constant foam density (≈ 35 kg/m^3) but different cell distributions (see Table 1). The morphology of the foams was characterized by image analysis of scanning electron microscopy (SEM) observations of foam specimens prepared by razor blade cutting. The morphology of the first series was characterized in the plane normal to the machine direction, designated as M-plane, and to the thickness direction, designated as T-plane. For the second series, the morphology in the plane normal to the lateral direction, designated as L-plane, was characterized in addition to the previous planes. A schematic of these plane designations is provided in Figure 1.

The cell size was calculated from the area of individual cells as the equivalent diameter of a circle. The cell size distribution, the number-average diameter d_n, the volume-average diameter d_v, and their ratio d_v/d_n, used as a measure of the cell dispersity, were obtained. A minimum count of 200 cells was employed for the determination of each cell size distribution.

Compression testing was performed according to ASTM D1621 [5] standard test method. For all tests, the thickness of the specimens was that of the as-received boards (between 25 and 50 mm). The tests were done at low (2.5 mm/min) and high (3 m/s) compression speeds. The low speed tests were performed using a computer-controlled Instron mechanical tester on specimens with a cross section of 50×50 mm^2. The high-speed tests were performed using an impact tower equipped with a displacement transducer and load cell on specimens with a cross section of 50×50 mm^2. The load–displacement curves were monitored

Table 1. Foam morphology (series 1: samples from Dow Chemical; series 2: samples from Sealed Air).

Series	Foam sample	ρ (kg/m^3)	Plane normal to:	d_n (μm)	$\rho/d \times 10^2$ (kg/m^3 μm^{-1})
1	1	28.5	M	1790	1.59
			T	1336	2.13
	2	38.7	M	971	3.99
			T	873	4.43
	3	64.4	M	883	7.29
			T	703	9.16
	4	102.0	M	602	16.94
			T	613	16.64
2	5	35.0	T	1044	3.35
			M	1492	2.35
			L	1601	2.19
	6	35.1	T	1401	2.51
			M	1879	1.87
			L	1845	1.90
	7	35.2	T	1027	3.43
			M	1293	2.72
			L	1588	2.22
	8	35.7	T	892	4.00
			M	1182	3.02
			L	1476	2.42

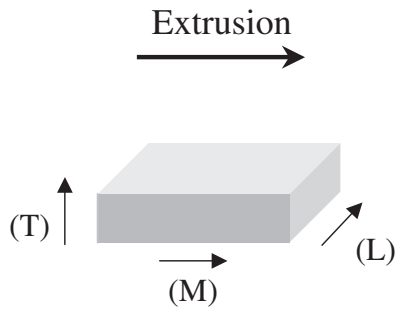

Figure 1. Schematic representation of the plane designation with respect to the extrusion or machine direction; the plane normal to the machine, thickness, and lateral directions are designated as M-, T-, and L-planes, respectively.

during these tests. The compressive modulus of elasticity and compressive stress at yield, defined as the transition between the linear and plateau regions of the load–displacement curves, were calculated according to ASTM D1621 for the low-speed tests, but only

the compressive stress at yield could be obtained with acceptable reproducibility for the high-speed tests.

RESULTS

The cell size dispersity ratio d_v/d_n, obtained from the characterization of the cell size distribution, was respectively 1.16 and 1.32 for foam series 1 and 2, i.e., relatively close to 1, which indicates that the cell size distribution is close to statistically perfectly normal. The number-average cell diameter was thus assumed to reflect the cell size distribution. The densities and cell sizes measured are listed in Table 1. These results show that the cell size varied between 0.6 and 1.9 mm and that ρ/d ranged between 0.016 and 0.170 $kg/m^3\,\mu m^{-1}$, i.e., slightly more than one decade. For the foams in series 1, the mean cell diameter is nearly the same in the two planes tested, with a trace of anisotropy detected with the decrease in the foam density. For the foams of series 2, huge anisotropy prevails, with the smaller cell diameters detected in the T-plane and the larger diameters observed in the L-plane. T-plane values of ρ/d are the highest and L-plane ρ/d-values the lowest, in general.

Figure 2 displays the density as a function of the mean cell size for all foams. In the hypothetical case that the density is proportional on a one-to-one basis with the reciprocal of the cell diameter, no improvement would be obtained through the use of Equations (3) and (4). However, as displayed in Figure 2, the data exhibit scatter that should be considered as additional information relevant to the use of a more complex model.

Low-speed compression tests on both foam series were performed. Examples of the compressive stress–strain curves obtained are shown in Figure 3 for two foams (samples #2 and #5) with almost the same density (35–38 kg/m^3), but different cell sizes. Despite the close densities considered in Figure 3, these curves and their associated compressive modulus of elasticity and yield stress differ significantly depending on the plane investigated and foam considered. These curves demonstrate the limitations of the Gibson–Ashby models (Equations (1) and (2)), which do not capture the specific morphological characteristics of foams, and cannot thus predict the resulting properties accurately. A confirmation of this is provided in Figure 4, in which the compressive modulus of elasticity and yield stress obtained from the compressive stress–strain curves are reported as a function of density. Figure 4 exhibits very important data scatter, and poor correlation factors ($r^2 \leq 0.3$) were obtained. This figure also indicates that, while properties increase with higher density, they cannot be expressed simply as a function of density but should also depend on other structural parameters of the foam.

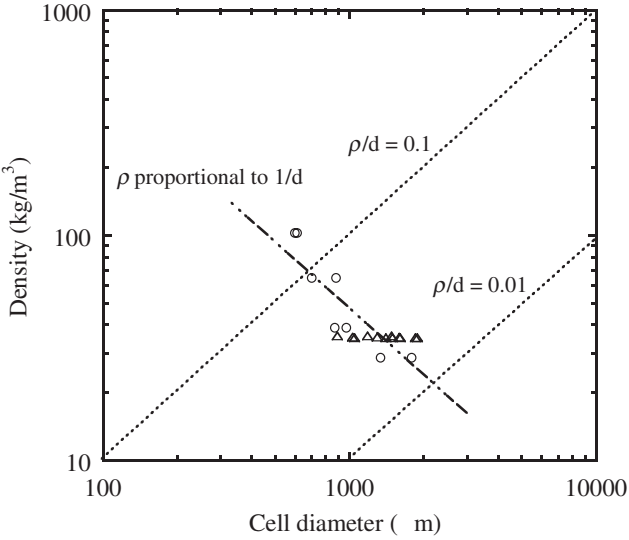

Figure 2. Foam density plotted against the mean cell diameter. Dotted lines correspond to typical ρ/d values covered in this work. Slash-dotted line illustrates the hypothetical 1 : 1 relationship between ρ and $1/d$.

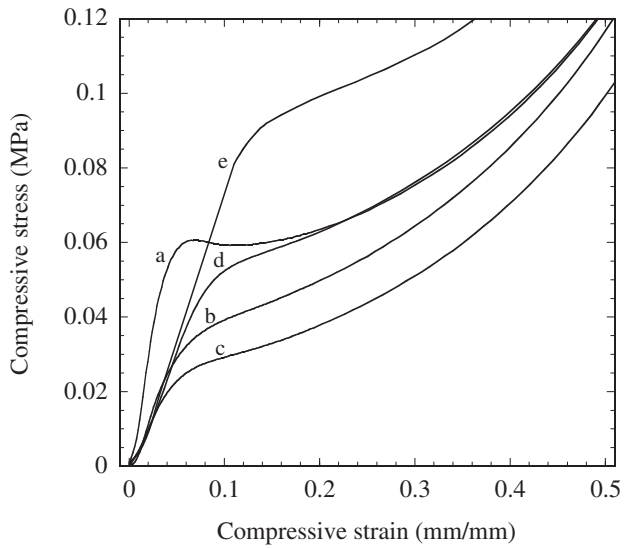

Figure 3. Typical compressive stress–strain curves for two PE foams; PE foam #5 (a) in T-direction; (b) in L-direction; and (c) in M-direction, and PE foam #2 (d) in T-direction and (e) in M-direction.

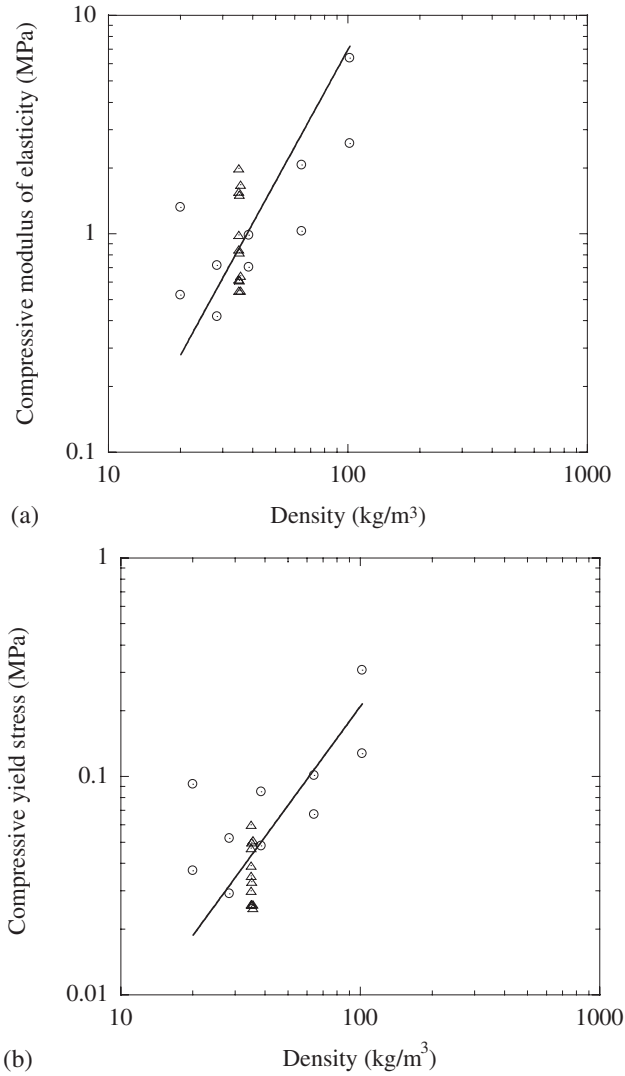

Figure 4. Low-speed compression test results of foam series 1 (○) and 2 (△) plotted against density: (a) compressive modulus of elasticity ($r^2 = 0.11$) and (b) compressive yield stress ($r^2 = 0.30$). The lines represent fits based on the simplified power-law Equations (1) and (2).

This is especially true for the data associated with the foam series 2, with the properties spanning along the y-axis over nearly half a decade.

To account for the foam morphology, the compressive modulus of elasticity and yield stress obtained from the compressive stress–strain

curves are reported in Figure 5 as a function of the microstructural parameter ρ/d. This figure shows that, while some scatter in the data remains, plotting the compressive properties according to Equations (3) and (4) results in improved data representation (correlation factors

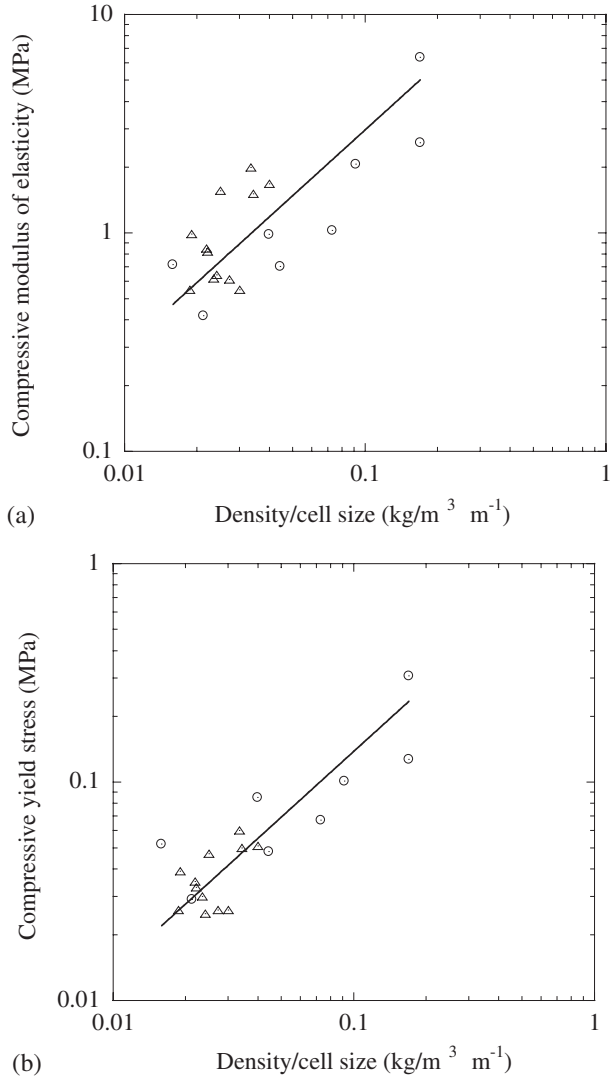

Figure 5. Low-speed compression test results of foam series 1 (○) and 2 (△) plotted against ρ/d: (a) compressive modulus of elasticity ($r^2 = 0.65$) and (b) compressive yield stress ($r^2 = 0.68$). The lines represent fits based on the power-law Equations (3) and (4).

$r^2 \geq 0.65$). This validates the use of Equations (3) and (4) based on ρ/d. Results from series 2 now display a trend sensitive to the cell diameter, with higher modulus and yield stress associated with foams having smaller cells. It is proposed that this approach should be used to correlate properties of foams, since it captures the essential characteristics of the foam morphology and provides properties prediction within an acceptable range of error. The success of this approach is especially interesting considering that no specific information regarding the exact PE matrix composition is available at this time.

To extend the validity of this approach to a wider range of testing conditions, high-speed compression tests were also performed. The results for the high-speed compressive stress at yield are shown in Figure 6 as a function of density. As observed previously in Figure 4, Figure 6 still exhibits very important data scatter, with lack of correlation for data from series 2.

Replacing the density by ρ/d to report the high-speed compressive stress at yield led to quite different results, as shown in Figure 7. In this case, a different power-law exponent of 0.5 had to be used for the linear regression based on Equation (4). This change in slope is related to a viscoelastic effect to which PE-based foams are subjected at room temperature, i.e., above their glass transition temperature, due to their rubbery state; higher values of yield stress are obtained at higher

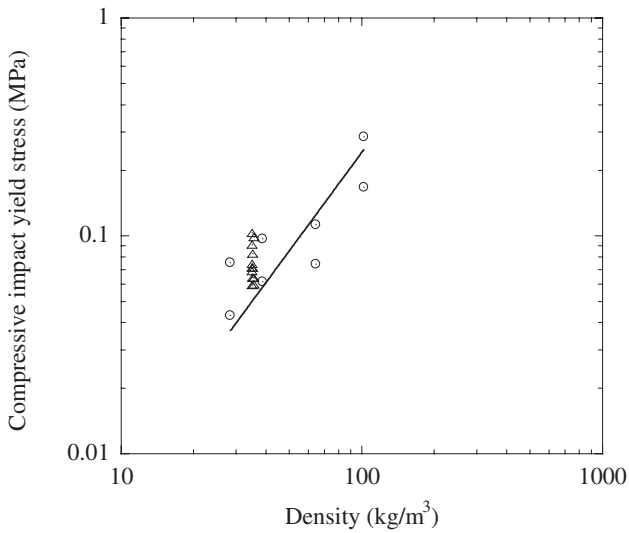

Figure 6. High-speed compressive stress at yield of foam series 1 (○) and 2 (△) plotted against density ($r^2 = 0.55$). The line represents fit based on the power-law Equation (2).

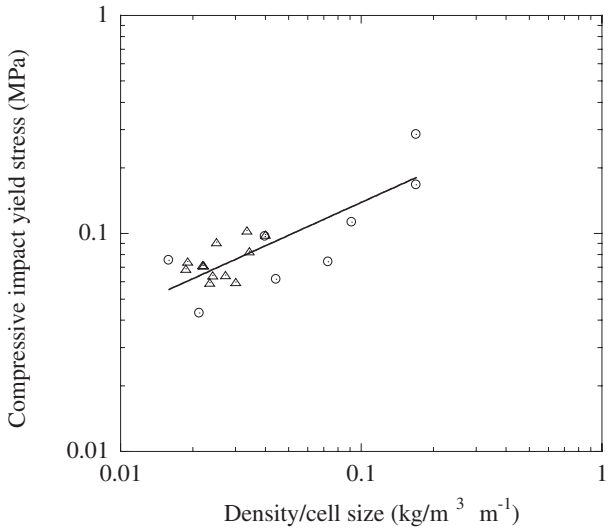

Figure 7. High-speed compression yield stress of foam series 1 (○) and 2 (△) plotted against ρ/d ($r^2 = 0.62$). The line represents fit based on the power-law Equation (4), with however an exponent of 0.5.

strain rates. While the correlation factor was not dramatically changed, its slight improvement is associated with the compressive stresses at yield for foams of series 2 exhibiting again a positive trend with the parameter ρ/d.

DISCUSSION

The results obtained from PE foams of two different series suggest that mechanical properties can be expressed as a function of ρ/d. Similar results were obtained and have been presented for closed-cell PS foams [3]. These PS foams had a density varying between 25 and 74 kg/m^3 and an average cell size between 78 and 231 μm. Since the results presented here were correlated using the same power-law relationships obtained in the previous study, both families of foams appear to follow the same trends with respect to ρ/d. The results obtained from the two studies are reported in Figure 8, with the mechanical properties and microstructural parameter extending over two decades, which shows graphically how well the properties of these different foams scale with ρ/d according to power-law relationships. This is confirmed by the good correlation factors obtained ($r^2 \geq 0.79$), considering the diversity in foams characteristics and properties: semi-crystalline and amorphous polymeric

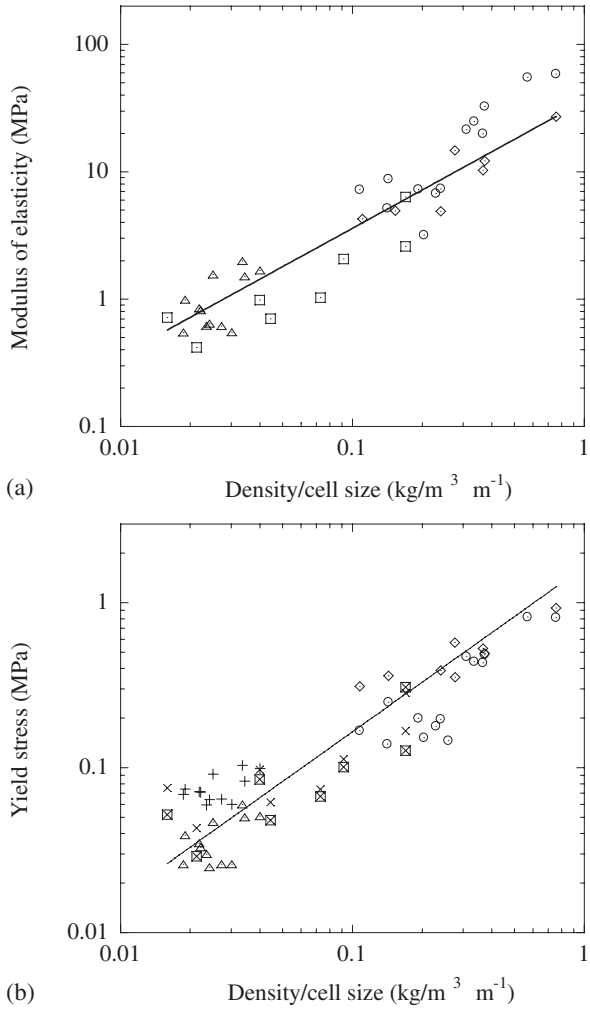

Figure 8. Mechanical properties of different foams and different conditions plotted against ρ/d: (a) modulus of elasticity ($r^2 = 0.87$) and (b) stress at yield ($r^2 = 0.79$) for PS foams (from [1]) from low-speed compression (○) and falling dart impact (◇) tests, PE foams series 1 from low-speed (□) and high-speed (×) compression tests, and PE foams series 2 from low-speed (△) and high-speed (+) compression tests. The lines represent fits based on the power-law Equations (3) and (4).

foams, with densities between 20 and 100 kg/m^3, cell sizes between 78 μm and 1.9 mm and various levels of anisotropy.

In light of the success of this approach, some general guidelines for foam processing might be suggested. The first is that the properties of

foams could be optimized by using the power-law regressions proposed in Equations (3) and (4). Foam properties at a given density could be enhanced by a reduction of the average cell size, or properties could be maintained at a lower density by reducing the cell size, to keep the microstructural parameter ρ/d constant. This indication provides support to MCFs, which show properties claimed to be maintained with respect to the unfoamed polymer for density reduction of typically 30%, as a result of a very fine cellular structure [4].

Provided that it is validated for a specific system, the correlation between the properties and the microstructural parameter ρ/d also indicates an opportunity in terms of material costs, since the same properties could be obtained for a lower density, i.e., for a smaller amount of materials. This effect of microstructure is not predicted in the Gibson–Ashby model (Equations (1) and (2)), since the latter only considers the relative density and thus predicts that lower amount of materials leads to lower properties. The Gibson-Ashby model should be considered as a macroscopic comparison tool between different foams, or even different materials, and not as a property predicting means.

CONCLUSIONS

The results in this study show that the compressive properties of PE foams, tested at low and high speeds (impact), cannot be successfully correlated using the Gibson–Ashby model, since the latter only considers the density as the sole parameter describing the foam. To account for the specific characteristics of the PE foams tested (densities between 28 and 102 kg/m^3, and average cell size between 600 and 1900 μm), a microstructural parameter, ρ/d, previously proposed for PS foams [3], was used instead of the density. The compressive modulus of elasticity and stress at yield of the PE foams could be expressed as a function of ρ/d, with good resulting correlation factors. This correlation of PE foams properties was extended to previously reported PS properties. The latter showed the validity of the proposed microstructural parameter ρ/d to reflect the morphology of foams of different nature, structure, and properties.

ACKNOWLEDGMENTS

The collaboration of Sealed Air (Dr. S.-T. Lee) and Dow Chemicals (Mr. Marty Tusim) for providing foam samples and the technical work of Nicole Côté and Martin-Alexandre Tanguay both at the National Research Council Canada for the microstructural and mechanical characterization are gratefully acknowledged.

REFERENCES

1. Gibson, L.J. and Ashby, M.F. (1997). *Cellular Solids Structure and Properties*, **2nd edn**, Cambridge University Press, Cambridge, 510 p.
2. Ashby, M.F. (1992). *Materials Selection in Mechanical Design*, **2nd edn**, Butterworth-Heinemann, Oxford, 311 p.
3. Bureau, M.N. and Gendron, R. (2003). Mechanical-Morphology Relationship of PS Foams, *J. Cell. Plast.*, **39**(5): 353–367.
4. Collias, D.I., Baird, D.G. and Borggreve, R.J.M. (1994). Impact Toughening of Polycarbonate by Microcellular Foaming, *Polymer*, **35**(18): 3978–3983.
5. American Society for Testing and Materials, ASTM D1621-00, *Standard Test Method for Compressive Properties of Rigid Cellular Plastics*.